AD-A174 432 THE BAUSCHINGER EFFECT ON STRESS INTENSITY FACTORS FOR A RADIALLY CRACKED GUN TUBE(U) ARMY CLOSE COMBAT ARMAMENTS CENTER WATERVLIET NY S L PU ET AL OCT 86 1/1

UNCLASSIFIED ARCCB-TR-86033 F/G 19/6 NL

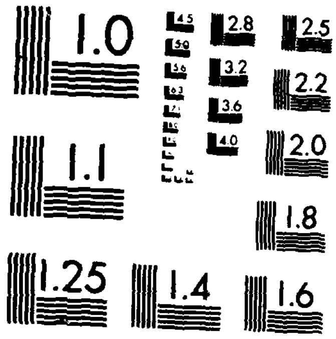

MICROCOPY RESOLUTION TEST CHART
NATIONAL BUREAU OF STANDARDS 1963-A

(12)

AD

AD-A174 432

TECHNICAL REPORT ARCCB-TR-86033

THE BAUSCHINGER EFFECT ON STRESS INTENSITY FACTORS FOR A RADIALLY CRACKED GUN TUBE

S. L. PU

P. C. T. CHEN

OCTOBER 1986

US ARMY ARMAMENT RESEARCH AND DEVELOPMENT CENTER
CLOSE COMBAT ARMAMENTS CENTER
BENÉT WEAPONS LABORATORY
WATERVLIET, N.Y. 12189-4050

DISCLAIMER

The findings in this report are not to be construed as an official Department of the Army position unless so designated by other authorized documents.

The use of trade name(s) and/or manufacturer(s) does not constitute an official indorsement or approval.

DESTRUCTION NOTICE

For classified documents, follow the procedures in DoD 5200.22-M, Industrial Security Manual, Section II-19 or DoD 5200.1-R, Information Security Program Regulation, Chapter IX.

For unclassified, limited documents, destroy by any method that will prevent disclosure of contents or reconstruction of the document.

For unclassified, unlimited documents, destroy when the report is no longer needed. Do not return it to the originator.

SECURITY CLASSIFICATION OF THIS PAGE (When Data Entered)

REPORT DOCUMENTATION PAGE

READ INSTRUCTIONS BEFORE COMPLETING FORM

1. REPORT NUMBER ARCCB-TR-86033	2. GOVT ACCESSION NO. AD-A174432	3. RECIPIENT'S CATALOG NUMBER
4. TITLE (and Subtitle) THE BAUSCHINGER EFFECT ON STRESS INTENSITY FACTORS FOR A RADIALLY CRACKED GUN TUBE		5. TYPE OF REPORT & PERIOD COVERED Final 6. PERFORMING ORG. REPORT NUMBER
7. AUTHOR(s) S. L. Pu and P. C. T. Chen		8. CONTRACT OR GRANT NUMBER(s)
9. PERFORMING ORGANIZATION NAME AND ADDRESS US Army Armament Research, Develop, & Engr Center Benet Weapons Laboratory, SMCAR-CCB-TL Watervliet, NY 12189-4050		10. PROGRAM ELEMENT, PROJECT, TASK AREA & WORK UNIT NUMBERS AMCMS No. 6111.02.H600.011 PRON No. 1A52F51D1A1A
11. CONTROLLING OFFICE NAME AND ADDRESS US Army Armament Research, Develop, & Engr Center Close Combat Armaments Center Dover, NJ 07801-5001		12. REPORT DATE October 1986 13. NUMBER OF PAGES 30
14. MONITORING AGENCY NAME & ADDRESS(if different from Controlling Office)		15. SECURITY CLASS. (of this report) UNCLASSIFIED 15a. DECLASSIFICATION/DOWNGRADING SCHEDULE

16. DISTRIBUTION STATEMENT (of this Report)

Approved for public release; distribution unlimited.

17. DISTRIBUTION STATEMENT (of the abstract entered in Block 20, if different from Report)

18. SUPPLEMENTARY NOTES

Presented at the Third Army Conference on Applied Mathematics and Computing, Georgia Institute of Technology, Atlanta, Georgia, 13-16 May 1985.
Published in Proceedings of the Conference.

19. KEY WORDS (Continue on reverse side if necessary and identify by block number)

Bauschinger Effect
Stress Intensity Factors
Radial Cracks
Thick-Wall Cylinders
Residual Stresses
Elastic-Plastic Unloading
Reverse Yielding

20. ABSTRACT (Continue on reverse side if necessary and identify by block number)

The theoretical predicted fatigue life of a high strength steel tube which has undergone an autofrettage procedure is significantly higher than the experimental prediction. To account for the discrepancy, attention is now turned to developing better elastic-plastic models for a high strength steel. An improved material model shows that reverse yielding may occur in the inner portion of the tube. This reverse yielding reduces the residual compressive
(CONT'D ON REVERSE)

20. ABSTRACT (CONT'D)

hoop stress considerably which has an adverse effect on bore crack propagation. This study considers the stress intensity factors due to a radial crack taking the Bauschinger effect into consideration.

The elastic-plastic interfaces during loading and unloading in the autofrettage process divide the tube into three-ring regions. The residual stress distribution in each region is quite different. When a crack grows from one region into another, the previous method using functional stress intensity fails. A new method is used to obtain stress intensity factors for a radial crack growing out of the reverse yielding zone. This approach is based on crack face weight functions obtained by Sha using stiffness derivative finite element techniques coupled with singular crack-tip elements.

TABLE OF CONTENTS

TABLES

LIST OF ILLUSTRATIONS

INTRODUCTION

An early brittle failure of a cannon tube during the 1960's prompted a renewed interest in fracture analysis of cannon pressure vessels (ref 1). After careful investigation of the cause of fracture, some basic design changes were made to prevent any further failures. One of the design changes was to introduce a compressive residual stress near the inner radius of the cannon by an autofrettage process. Considerable efforts have been made to predict the residual stress distribution in an overstrained tube based on various material models (refs 2-5). In order to confirm the theoretical predictions of residual stresses, experimental methods (refs 6,7) have been initiated in our laboratory.

Since the current cannon tube design uses a wall ratio close to two, the maximum compressive residual stress at the bore for a fully autofrettaged tube is about 85 percent of the yield stress σ_0 of the material. Most of the earlier predictions of residual stresses were based on the assumption of elastic unloading. According to Milligan et al (ref 8), the high strength gun steel has a very high Bauschinger effect. To account for the compressive yield strength reduction due to the Bauschinger effect, Underwood and Kendall (ref 9) have tried to estimate the residual stress distribution and its effect on fatigue crack growth rate. Recently, Chen obtained a closed form solution of residual stresses in autofrettaged tubes based on a theoretical material model taking both Bauschinger and hardening effects into consideration (ref 10). The new residual stress distribution is very different from that

References are listed at the end of this report.

obtained earlier based on the assumption of elastic unloading. The functional stress intensity method developed for the computation of stress intensity factors of a radial crack initiating from the inner radius of a tube may fail due to the presence of a reverse yielding region near the bore. The objective of this report is to develop a numerical method to overcome such a difficulty and to study the Bauschinger effect on stress intensity factors for a radially cracked, partially autofrettaged gun tube.

THE BAUSCHINGER EFFECT AND RESIDUAL STRESSES

The phenomenon that a material lowers its elastic limit in compression (tension) subsequent to a previous stressing in tension (compression) beyond the elastic limit is called the Bauschinger effect. A quantity representing the magnitude of the Bauschinger effect is the Bauschinger effect factor (BEF). This is defined as the ratio of the yield stress upon reverse loading to the initial yield stress (σ_0). The BEF (f) is a function of percent overstrain ($_{\varepsilon}P$). The graph of BEF versus percent overstrain obtained by Milligan et al (ref 8) for a modified 4330 steel having a martensitic structure is shown in Figure 1 which was used by Chen in his computations of residual stresses.

Taking the Bauschinger effect factor f into consideration, Chen obtained the closed form solution of residual stresses in autofrettaged tubes (ref 10). He assumed a material model which exhibits the stress-strain curve shown in Figure 2 during tensile loading and unloading after overstrain. The assumption of elastic-perfectly plastic loading was supported by the fact that very little strain-hardening was observed in the tensile test. A bilinear model for elastic-plastic unloading was assumed since a large slope of strain-hardening ($m'E$) did develop after the occurrence of reverse yielding.

Referring to the point O' in Figure 2 as the origin of a new (primed) coordinate system (σ', ε'), the reverse yielding curve can be expressed as

$$\frac{\sigma'}{\sigma_o} = 1 + f + m'\zeta/(1-m') \tag{1}$$

where $\zeta = (E/\sigma_o)\varepsilon'^P$, E is Young's modulus, and ε'^P is the plastic strain in the primed coordinates. The final residual stress state (denoted by a double prime) is obtained by summing the stress state corresponding to the elastic-perfectly plastic loading and the primed stress state corresponding to unloading. The tangential and radial components can be written as

$$\sigma_\theta'' = \sigma_\theta + \sigma_\theta' \quad , \quad \sigma_r'' = \sigma_r + \sigma_r' \tag{2}$$

Elastic-Plastic Loading

Let a and b be the inner and outer radii of the cylinder, respectively, and let the material be elastic-perfectly plastic, obeying Tresca's yield criterion. The stress components are given in Reference 2 as follows:

$$\begin{matrix} \sigma_r/\sigma_o \\ \sigma_\theta/\sigma_o \end{matrix} = \frac{1}{2}\left(\mp 1 + \frac{\rho^2}{b^2}\right) - \ln\frac{\rho}{r} \quad , \quad a < r < \rho \tag{3}$$

$$\begin{matrix} \sigma_r/\sigma_o \\ \sigma_\theta/\sigma_o \end{matrix} = \frac{1}{2}\left(\frac{\rho^2}{b^2} \mp \frac{\rho^2}{r^2}\right) \quad , \quad \rho < r < b \tag{4}$$

where ρ is the elastic-plastic boundary relating to the internal pressure p by

$$\frac{p}{\sigma_o} = \frac{1}{2}\left(1 - \frac{\rho^2}{b^2}\right) + \ln\left(\frac{\rho}{a}\right) \tag{5}$$

The equivalent plastic strain can be calculated by

$$\frac{E}{\sigma_o} \varepsilon^p = \beta_1 \left(\frac{\rho^2}{r^2} - 1\right) \quad , \quad a \le r \le \rho \tag{6}$$

where

$$\beta_1 = \frac{2}{\sqrt{3}} (1-\nu^2) \tag{7}$$

In Eq. (7) ν is Poisson's ratio.

Elastic-Plastic Unloading

If the internal pressure p is subsequently removed completely, the unloading may be either elastic or elastic-plastic depending on whether the magnitude of p is less than or greater than p_m which is the minimum pressure to cause the reverse yielding to occur. If $p \le p_m$, the unloading is entirely elastic and the stress components are

$$\begin{matrix}\sigma_r' \\ \sigma_\theta'\end{matrix} = \frac{p}{\frac{b^2}{a^2} - 1} \left[\pm \frac{b^2}{r^2} - 1\right] \tag{8}$$

Using Tresca's criterion subject to $\sigma_r'' > \sigma_z'' > \sigma_\theta''$, the reverse yielding will not occur if

$$\sigma_r'' - \sigma_\theta'' \le f\sigma_o \tag{9}$$

Substituting Eqs. (2), (3), and (8) into Eq. (9), we obtain the expression for p_m

$$\frac{p_m}{\sigma_o} = \frac{1}{2} (1+f)\left(1 - \frac{a^2}{b^2}\right) \tag{10}$$

If $p > p_m$, reverse yielding will occur in a region $a \le r < \rho'$ with $\rho' < \rho$ upon unloading and we have from Eq. (1)

$$\sigma_r'' - \sigma_\theta'' = f\sigma_o + m'E\varepsilon'^p/(1-m') \quad \text{in} \quad a \le r < \rho' \tag{11}$$

The stresses in the plastic and elastic regions are given by Bland (ref 3) as

$$\sigma_r'/\sigma_o = p/\sigma_o - \frac{1}{2}\beta_2'(1+f)(\frac{\rho'}{a})^2(1-\frac{a^2}{r^2}) - (1-\beta_2')(1+f)\ln(\frac{r}{a}) \quad , (a<r<\rho') \tag{12}$$

$$\sigma_\theta'/\sigma_o = \sigma_r'/\sigma_o - (1+f) - m'\zeta'/(1-m') \; , (a<r<\rho') \tag{13}$$

$$\left.\begin{matrix}\sigma_r'/\sigma_o \quad (14)\\ \sigma_\theta'/\sigma_o \quad (15)\end{matrix}\right\} = \frac{1}{2}(1+f)[\pm(\frac{\rho'}{r})^2 - (\frac{\rho'}{b})^2] \; , \quad (\rho'<r<b)$$

where

$$\beta_1' = (1-m')/[m'+(1-m')/\beta_1] \tag{16}$$

$$\beta_2' = m'\beta_1'/(1-m') \tag{17}$$

$$\zeta' = \beta_1'(1+f)(\rho'^2/r^2-1) \tag{18}$$

The value of ρ' can be found from continuity of σ_r' at ρ' from Eqs. (12) and (14). Figure 3 shows different residual hoop stress distributions for a hollow cylinder with a wall ratio of two and $E/\sigma_o = 200$, $\nu = 0.3$, $\rho/a = 1.6$ and 2.0. The broken lines are elastic unloading solutions (f=1), while the solid lines are elastic-plastic unloading with $m' = 0$ and 0.3. The figure shows a drastic difference in σ_θ'' in the reverse yielding region near the bore and it shows that ρ' varies slightly with ρ and m'.

FUNCTIONAL STRESS INTENSITY METHOD

We have developed the functional stress intensity method (ref 11) for the computation of stress intensity factors of radial cracks in a pressurized and partially autofrettaged cylinder by combining the finite element method and the weight function method. A weight function vector $\underline{h}$ is a universal function which depends only on geometry and not on loadings (ref 12). For a given radially cracked ring, if $K_I^{(1)}$, the mode I stress intensity factor, and

$v^{(1)}$, the normal component of crack face displacement associated with a symmetric load system 1, are known, then the normal component of the crack face weight functions can be expressed by

$$h_{Iy}(x,\ell) = \frac{H}{2K_I^{(1)}} \frac{\partial v^{(1)}(x,\ell)}{\partial \ell} \tag{19}$$

where $H = E$ for plane stress and $H = E/(1-\nu^2)$ for plane strain, $x = (r-a)$ is a distance measured from the base of the crack along the crack face toward the crack tip, and ℓ is the crack length. For any symmetric load applied to the same cracked ring, the stress intensity factor associated with the new load can be found from

$$K_I = \frac{H}{K_I^{(1)}} \int_o^\ell p(x) \frac{\partial v^{(1)}}{\partial \ell} dx \tag{20}$$

where $p(x)$ is the normal stress in the tangential direction at the crack site due to the new load applied to the uncracked ring. If the uniform tension p_o at the outer radius is taken as load one, we can find numerical values of $K_I^{(1)}$ and $v^{(1)}$ by the finite element method. We wish to use Eq. (20) to obtain K_I associated with the autofrettage residual stresses. It can be seen from Eqs. (2), (3), (8), and (12) through (15) that the residual stress σ_θ'' has the general expression

$$\sigma_\theta''(r) = A_1 + A_2/r^2 + A_3 \ln(r) \tag{21}$$

for a tube subject to an elastic-plastic loading prior to an elastic unloading, where A_i, $i = 1,2,3$ are superposition constants.

Let $p(x)$ in Eq. (20) be σ_θ'' above. The integration to find K_I requires an expression for $\partial v^{(1)}/\partial \ell$. A method which assumes $v^{(1)}$ as a conic section (ref 13) has been used by Grandt (ref 14). Another method which avoids the need of $\partial v^{(1)}/\partial \ell$ has been developed by Pu (ref 11). He uses finite elements to obtain functional stress intensities $K_c(1)$, $K_c(r^{-2})$, and $K_c(\ell n r)$ defined by

$$K_c(p) = \frac{H}{K(1)} \int_o^{\ell} p \frac{\partial v^{(1)}}{\partial \ell} dx \tag{22}$$

for a crack face loading $p = 1$, $p = r^{-2}$, and $p = \ell n(r)$, respectively. Once the functional stress intensities are known, then the stress intensity factor $K_I(p)$ can be found for a general residual stress distribution of Eq. (21) by an algebraic equation

$$K_I(p) = A_1K_c(1) + A_2K_c(r^{-2}) + A_3K_c(\ell nr) \tag{23}$$

This method was successfully applied to various residual stresses predicted from various material models (ref 15).

Nc· for a radial crack in a reverse yielding zone, the stress intensity factor can still be found by the functional stress intensity method since the residual stress remains the same form as Eq. (21) with the superposition constants obtainable from Eqs. (3) and (13). However, if the radial crack is longer than the reverse yielding zone, the functional stress intensity method fails since the crack face loading p(x) has two different expressions in two different regions: $0 < x < \rho'-a$ and $\rho'-a < x < \ell$. Let $p_Y(x)$ and $p_e(x)$ be the crack face loading (residual hoop stress) in the reverse yielding region and the elastic region. Equation (20) becomes

$$K_I = 2\int_o^{\rho'-a} p_Y(x)h_{Iy}(x,\ell)dx + 2\int_{\rho'-a}^{\ell} p_e(x)h_{Iy}(x,\ell)dx \tag{24}$$

To use this equation, we have to find the explicit crack face weight function h_{Iy} using the stiffness derivative finite element technique explained in the next section.

EXPLICIT CRACK FACE WEIGHT FUNCTION

The stiffness derivative method for determining linear elastic stress intensity factors was introduced by Parks (ref 16). The method was extended to calculate the weight function vector field by Parks and Kamenetzky (ref 17). An efficient finite element evaluation of explicit weight functions has been established by Sha (ref 18) who combined the stiffness derivative technique with special singular crack-tip elements. He and Yang applied the method to radial crack problems of a hollow disk (ref 19). The degenerated quarter-point quadratic elements were used around a crack tip. These singular elements were surrounded by the standard eight-node quadrilateral elements. The virtual crack extension of an amount $\delta\ell$ was simulated by advancing the crack-tip node by $\delta\ell$ in the direction colinear with the mode I radial crack (x-direction). The surrounding quarter-point nodes were also shifted to new locations and there was no change in location of all other nodes. Hence only a few crack-tip elements have experienced changes in elemental stiffness due to the virtual crack extension. This makes the stiffness derivative technique very efficient from a computational viewpoint.

From the displacement form of the finite element method, the equation of equilibrium is

$$[K]\{u\} = \{F\} \tag{25}$$

where [K] is the global sitffness matrix, and {u} and {F} are displacement vector and load vector, respectively. The change in displacement per unit crack extensions can be found by differentiating Eq. (25) with respect to crack length ℓ

$$\frac{d\{u\}}{d\ell} = [K]^{-1}\left[\frac{d\{F\}}{d\ell} - \frac{d[K]}{d\ell}\{u\}\right] \tag{26}$$

Note that $d\{F\}/d\ell = 0$ if we select a load system which consists of only surface tractions not applied on the crack face. The global stiffness derivative $d[K]/d\ell$ is the sum of N_c elemental stiffness derivatives

$$\frac{d[K]}{d\ell} = \sum_{i=1}^{N_c} \frac{d[k_i]}{d\ell} \tag{27}$$

where N_c is the number of crack-tip elements and $[k_i]$ is the element stiffness of the i^{th} crack-tip element. For a small crack extension $\delta\ell$, the element stiffness derivative may be approximated by

$$\frac{d[k_i]}{d\ell} = \frac{[k_i]_{\ell+\delta\ell} - [k_i]_{\ell}}{\delta\ell} \tag{28}$$

where $[k_i]_{\ell+\delta\ell}$ and $[k_i]_{\ell}$ are element stiffness after and before virtual crack extension, respectively.

The displacement vector is a function of position (x,y) and the crack length ℓ as follows:

$$\{u\} = \{u(x,y,\ell)\} \tag{29}$$

Applying the chain rule of differentiation of Eq. (29) with respect to ℓ gives

$$\frac{\partial\{u\}}{\partial\ell} = \frac{d\{u\}}{d\ell} - \frac{\partial\{u\}}{\partial x}\frac{dx}{d\ell} - \frac{\partial\{u\}}{\partial y}\frac{dy}{d\ell} \tag{30}$$

For a mode I crack lying on the x-axis with colinear virtual crack extension, we have $dx/d\ell = 1$ and $dy/d\ell = 0$. Definitions of global coordinates and displacements for isoparametric elements are

$$x = \sum N_i(\xi,\eta)x_i \quad , \quad u = \sum N_i(\xi,\eta)u_i$$
$$y = \sum N_i(\xi,\eta)y_i \quad , \quad v = \sum N_i(\xi,\eta)v_i \tag{31}$$

where ξ,η are local coordinates; x,y are global coordinates; x_i,y_i are global coordinates of node i; u_i and v_i are x and y components of displacement at node i; $N_i(\xi,\eta)$ are shape functions which interpolate the displacement over the element. The finite element evaluation of $\partial\{u\}/\partial x$ can be carried out from

$$\frac{\partial\{u\}}{\partial x} = \frac{1}{\det[J]} \left\{\frac{\partial[N_i u_i]}{\partial\xi}\frac{\partial y}{\partial\eta} - \frac{\partial[N_i u_i]}{\partial\eta}\frac{\partial y}{\partial\xi}\right\} \tag{32}$$

where [J] is the Jacobian matrix. This leads to the expression for the y component of mode I weight function vector at (x,y)

$$h_{Iy}(x,y,\ell) = \frac{H}{K_I^{(1)}(\ell)} \left[\frac{dv^{(1)}}{d\ell} - \frac{1}{\det[J]} \left\{\frac{\partial[N_i u_i]}{\partial\xi}\frac{\partial y}{\partial\eta} - \frac{\partial[N_i u_i]}{\partial\xi}\frac{\partial y}{\partial\xi}\right\}\right] \tag{33}$$

For a hollow disk of $b/a = 2$, Sha and Yang [19] have obtained explicit weight functions for a single bore or rim radial crack. In a private communication, Sha has provided the following expression to approximate the dimensionless crack face weight function component

$$2\sqrt{\ell}\, h_{Iy}\left(\frac{r_s}{\ell}\right) = \sum_{n=1}^{4} D_n\left(\frac{r_s}{\ell}\right)^{n/2-1} \tag{34}$$

where r_s, the distance from the crack tip along the crack face, is related to x and r by

$$r_s = \ell - x = \ell + a - r \tag{35}$$

The coefficients D_n, $n = 1,2,3,4$, determined by the least squares technique, are given in the following table for various crack lengths.

TABLE 1. LEAST SQUARES FITTED COEFFICIENTS OF EQUATION (34) FOR A SINGLE BORE CRACK IN A HOLLOW CYLINDER OF b/a = 2 WITH VARIOUS CRACK LENGTHS c = ℓ/(b-a)

$\frac{\ell}{b-a}$	D_1	D_2	D_3	D_4
0.01	0.7966D+00	-0.7721D-02	0.2935D+00	0.3620D+00
0.02	0.7976D+00	-0.6980D-02	0.2840D+00	0.3608D+00
0.03	0.8130D+00	-0.7176D-01	0.3711D+00	0.3134D+00
0.05	0.8008D+00	-0.5811D-02	0.2649D+00	0.3551D+00
0.06	0.8335D+00	-0.1714D+00	0.4942D+00	0.2421D+00
0.08	0.8051D+00	-0.2789D-01	0.3116D+00	0.3270D+00
0.10	0.8286D+00	-0.1818D+00	0.6119D+00	0.1554D+00
0.20	0.8132D+00	-0.8254D-01	0.5769D+00	0.2414D+00
0.30	0.8026D+00	0.1409D-02	0.5881D+00	0.3756D+00
0.40	0.7981D+00	0.4661D-01	0.6908D+00	0.4935D+00
0.50	0.7956D+00	0.7236D-01	0.9065D+00	0.5437D+00
0.60	0.7990D+00	0.4395D-01	0.1361D+01	0.4059D+00
0.70	0.8004D+00	0.2255D-01	0.2130D+01	-0.3915D-01
0.80	0.7976D+00	0.4388D-01	0.3537D+01	-0.1131D+01

STRESS INTENSITY FACTORS

To use Eqs. (34) and (24), we need a certain transformation of variables. Let us use a, the bore radius, to normalize all linear lengths and use the same notations (before normalization) to denote the normalized lengths except that a is unit and b is w, the wall ratio. Denoting r_s/ℓ by τ in Eq. (34), then Eq. (24) associated with the residual hoop stress becomes

$$\frac{K_I}{\sigma_o\sqrt{\ell}} = \int_{\tau'}^{1} \left(\frac{\sigma_\theta''}{\sigma_o}\right)_Y \left(\sum_{n=1}^{4} D_n \tau^{n/2-1}\right) d\tau + \int_{o}^{\tau'} \left(\frac{\sigma_\theta''}{\sigma_o}\right)_e \left(\sum_{n=1}^{4} D_n \tau^{n/2-1}\right) d\tau$$

$$= \int_{o}^{1} \left(\frac{\sigma_\theta''}{\sigma_o}\right)_e \left(\sum_{n=1}^{4} D_n \tau^{n/2-1}\right) d\tau + \int_{\tau''}^{1} \left[\left(\frac{\sigma_\theta''}{\sigma_o}\right)_Y - \left(\frac{\sigma_\theta''}{\sigma_o}\right)_e\right]\left[\sum_{n=1}^{4} D_n \tau^{n/2-1}\right] d\tau \qquad (36)$$

where $(\sigma_\theta''/\sigma_o)_e$ is the residual hoop stress in the elastic unloading region, while $(\sigma_\theta''/\sigma_o)_Y$ is that in the reverse yielding region and τ' is the value of τ corresponding to $r = \rho'$, the elastic-plastic interface during unloading. The residual hoop stress can be represented by the general form

$$\left(\frac{\sigma_\theta''}{\sigma_o}\right)_e = A_{1e} + A_{2e}\, r^{-2}(\tau) + A_{3e}\, \ell n(r/\tau) \qquad (37)$$

$$\left(\frac{\sigma_\theta''}{\sigma_o}\right)_Y = A_{1Y} + A_{2Y}\, r^{-2}(\tau) + A_{3Y}\, \ell n(r/\tau) \qquad (38)$$

where the coefficients $A_{1e},\ldots,A_{3Y}$, can be obtained from Eqs. (2), (3), and (12) through (15). From Eq. (35) and the definition of τ, we have

$$r(\tau) = \ell(\ell_o - \tau) \quad , \quad \ell_o = (1+\ell)/\ell \qquad (39)$$

Denoting $I_{1n}(\alpha,\beta)$, $I_{2n}(\alpha,\beta)$, and $I_{3n}(\alpha,\beta)$ as the following definite integrals,

$$I_{1n}(\alpha,\beta) = \int_\alpha^\beta \tau^{n/2-1} d\tau$$

$$I_{2n}(\alpha,\beta) = \int_\alpha^\beta r^{-2}(\tau)\,\tau^{n/2-1} d\tau \qquad n = 1,2,3,4 \tag{40}$$

$$I_{3n}(\alpha,\beta) = \int_\alpha^\beta \ln(r(\tau))\,\tau^{n/2-1} d\tau$$

Eq. (36) can be written in the form

$$\frac{K_I}{\sigma_o\sqrt{\pi\ell}} = \frac{1}{\sqrt{\pi}} [\sum_{i=1}^{3} A_{ie} \sum_{n=1}^{4} D_n I_{in}(0,1) + \sum_{i=1}^{3} (A_{iY}-A_{ie}) \sum_{n=1}^{4} D_n I_{in}(\tau',1) \tag{41}$$

The expressions of integrals $I_{in}(\alpha,\beta)$, $i = 1,2,3$, $n = 1,\ldots 4$, are given in the Appendix. Equation (41) can be used for any loading which yields a hoop stress of the form given by Eq. (21) and for any multiple-cracked cylinder as long as the coefficients D_n are known for that particular cracked geometry. In case there is no reverse yielding region, Eq. (41) reduces to

$$\frac{K_I}{\sigma_o\sqrt{\pi\ell}} = \frac{1}{\sqrt{\pi}} \sum_{i=1}^{3} A_{ie} \sum_{n=1}^{4} D_n I_{in}(0,1) \tag{42}$$

For a shallow crack which lies entirely in the reverse yielding region, Eq. (41) becomes

$$\frac{K_I}{\sigma_o\sqrt{\pi\ell}} = \frac{1}{\sqrt{\pi}} \sum_{i=1}^{3} A_{iY} \sum_{n=1}^{4} D_n I_{in}(0,1) \tag{43}$$

Table 1 gives D_n for a single bore crack of various discrete crack lengths. For a crack length not given in Table 1, Sha and Yang (ref 19) suggested the use of cubic spline interpolation to obtain the weight function for that length from discrete values in Table 1 followed by the least squares technique to calculate D's.

Equation (42) is used to compute $K_I/p_o\sqrt{\pi \ell}$ for a single bore crack in a hollow cylinder of $w = 2$ subject to uniform tension p_o at the outside cylindrical surface. The Lamé solution gives $A_1 = A_2 = w^2/(w^2-1)$ and $A_3 = 0$.

Numerical results for various crack lengths are very accurate in comparison with results previously reported in Reference 20. A further check of numerical computations of $K_I/\sigma_o\sqrt{\pi \ell}$ from Eq. (42) has been done for a partially autofrettaged cylinder without reverse yielding. The results confirm those published in Reference 21.

For a cylinder of $w = 2$, the Bauschinger effect factors for 60 percent, 80 percent, and 100 percent overstrain are, from Figure 1, $f = 0.44$, 0.42, and 0.38, respectively. Using $\nu = 0.3$, $E/\sigma_o = 200$, the elastic-plastic interface ρ' during unloading depends on f and m'. It varies from $\rho' = 1.106$ for $\varepsilon = 0.6$ ($f = 0.44$) and $m' = 0.3$ to $\rho' = 1.20$ for $\varepsilon = 1$ ($f = 0.38$) and $m' = 0$. The residual hoop stress distributions near the bore for these two cases are shown in solid lines in Figure 3 while broken lines are corresponding stresses without taking Bauschinger effect into consideration. The residual stress in the reverse yielding region varies drastically with f and m'. Stress intensity factors due to residual stresses are calculated from Eq. (43) or (41) depending on whether the crack tip is inside or outside of the reverse yielding zone. Figures 4 and 5 are graphs of $K_I/(\sigma_o\sqrt{\pi \ell})$ as a function of dimensionless crack length $c = \ell/(w-1)$ for $\varepsilon = 0.6$ and $\varepsilon = 1$, respectively. Superposing stress intensity factors due to an internal pressure $p = \sigma_o/L_f$, the combined stress intensity factors from both p and residual stresses are shown in Figures 6 and 7 for $L_f = 3$ and for $\varepsilon = 0.6$ and $\varepsilon = 1.0$, respectively.

Figure 8 is a similar graph for $L_f = 1.5$ and $\varepsilon = 1.0$. In Figures 6, 7, and 8, the curves in the centerline correspond to $m' = 0$, the curves in the broken line are for $m' = 0.3$, while the solid lines are results obtained earlier without taking reverse yielding into consideration. For $c = 0.01$, Figure 7, values of $K_I/(\sigma_o\sqrt{\pi\ell})$ are 0.55 and 0.37 for $m' = 0$ and 0.3, respectively, versus the corresponding value 0.058 from the solid line. This indicates the Bauschinger effect will greatly reduce the advantageous effect of compressive residual hoop stress introduced by the autofrettage process.

CONCLUSION

The Bauschinger effect of the high strength gun steel causes the presence of the reverse yielding in a partially autofrettaged cannon tube of wall ratio of two. This reverse yielding reduces the magnitude of compressive hoop stress considerably in the reverse yielding region. This stress reduction will result in much higher stress intensity factors in a shallow bore crack in a pressurized and autofrettaged gun tube. The higher the stress intensity factor implies the lower the fatigue life.

The expression in Eq. (34) for explicit crack face weight function obtained by a combination of stiffness derivative technique and special singular crack-tip elements is highly accurate. It recovers the previous stress intensity factor results for a single bore crack in a tube subject to various loading conditions. The method can treat any crack face loading including stress discontinuities and stress gradient discontinuities over the crack face.

Numerical results here are limited to single bore radial cracks. However, the method is general for either bore cracks or rim cracks for any number of cracks as long as we have obtained the explicit crack face weight function for that particular cracked geometry.

REFERENCES

1. Davidson, T. E., Throop, J. F., and Underwood, J. H., "Failure of a 175 mm Cannon Tube and the Resolution of the Problem Using an Autofrettage Design," Case Studies in Fracture Mechanics, T. P. Rich and D. J. Cartwright, Eds., AMMRC MS77-5, Army Materials and Mechanics Research Center, 1977, pp. 1-13.
2. Koiter, W. T., "On Partially Plastic Tubes," C. B. Biezeno Anniversary Volume on Applied Mechanics, N.V. de Technische Uitgeverij, H. Stam. Haarlem, 1953.
3. Bland, D. R., "Elastoplastic Thick-Walled Tubes of Work-Hardening Materials Subject to Internal and External Pressures and Temperature Gradients," Journal of Mechanics and Physics of Solids, Vol. 4, 1956, pp. 209-229.
4. Chen, P. C. T., "The Finite Element Analysis of Elastic-Plastic Thick-Walled Tubes," Proceedings of Army Symposium on Solid Mechanics, The Role of Mechanics in Design-Ballistic Problems, 1972, pp. 243-253.
5. Chen, P. C. T., "Numerical Prediction of Residual Stresses in an Autofrettaged Tube of Compressible Material," Proceedings of the 1981 Army Numerical Analysis and Computer Conference, pp. 351-362.
6. Capsimalis, G. P., Haggerty, R. F., and Loomis, K., "Computer Controlled X-Ray Stress Analysis for Inspection of Manufactured Components," Technical Report WVT-TR-77001, Watervliet Arsenal, Watervliet, NY, 1977.
7. Frankel, J., Scholz, W., Capsimalis, G., and Korman, W., "Residual Stress Measurement in Circular Steel Cylinder," ARDC Technical Report ARLCB-TR-84018, Benet Weapons Laboratory, Watervliet, NY, 1984.

8. Milligan, R. V., Koo, W. H., and Davidson, T. E., "The Bauschinger Effect in a High-Strength Steel," Journal of Basic Engineering, Vol. 88, 1966, pp. 480-488.

9. Underwood, J. H. and Kendall, D. P., "Fracture Analysis of Thick-Wall Cylinder Pressure Vessels," Theoretical and Applied Fracture Mechanics, Vol. 2, 1984, pp. 47-58.

10. Chen, P. C. T., "The Bauschinger and Hardening Effect on Residual Stresses in an Autofrettaged Thick-Walled Cylinder," Journal of Pressure Vessel Technology, Vol. 108, February 1986, pp. 108-112.

11. Pu, S. L., "A Functional Stress Intensity Approach to Multiply Cracked, Partially Autofrettaged Cylinders," Transactions of the Twenty-Eighth Conference of Army Mathematicians, ARO Report 83-1, 1983, pp. 263-283.

12. Rice, J. R., "Some Remarks on Elastic Crack-Tip Stress Fields," Int. Journal of Solids and Structures, Vol. 8, 1972, pp. 751-758.

13. Orange, T. W., "Crack Shapes and Stress Intensity Factors For Edge-Cracked Specimens," ASTM STP 513, 1972, pp. 71-78.

14. Grandt, A. F., "Two Dimensional Stress Intensity Factor Solutions For Radially Cracked Rings," Technical Report AFML-TR-75-121, Air Force Materials Laboratory, 1975.

15. Pu, S. L. and Chen, P. C. T., "Stress Intensity Factors For Radial Cracks in a Prestressed Thick-Walled Cylinder of Strain-Hardening Materials," Journal of Pressure Vessel Technology, Vol. 105, No. 2, 1983, pp. 117-123.

16. Parks, D. M., "A Stiffness Derivative Finite Element Technique For Determination of Crack Tip Stress Intensity Factors," International Journal of Fracture, Vol. 10, No. 4, 1974, pp. 487-502.

17. Parks, D. M. and Kamenetzky, E. M., "Weight Functions From Virtual Crack Extension," International Journal for Numerical Methods in Engineering, Vol. 14, 1979, pp. 1693-1706.

18. Sha, George T., "Stiffness Derivative Finite Element Technique to Determine Nodal Weight Functions With Singularity Elements," Engineering Fracture Mechanics, Vol. 19, No. 4, 1984, pp. 685-699.

19. Sha, George T. and Yang, Chien-Tung, "Weight Functions of Radial Cracks in Hollow Disks," Presented at ASME 1985 Gas Turbine Conference in Houston, Texas, 1985.

20. Pu, S. L. and Hussain, M. A. "Stress Intensity Factors For a Circular Ring With Uniform Array of Radial Cracks Using Cubic Isoparametric Singular Elements," Fracture Mechanics, ASTM STP 677, 1979, pp. 685-699.

21. Pu, S. L. and Hussain, M. A., "Stress Intensity Factors For Radial Cracks in a Partially Autofrettaged Thick-Wall Cylinder," Fracture Mechanics, Fourteenth Symposium - Vol. 1: Theory and Analysis, ASTM STP 791, 1983, pp. I-194-I-215.

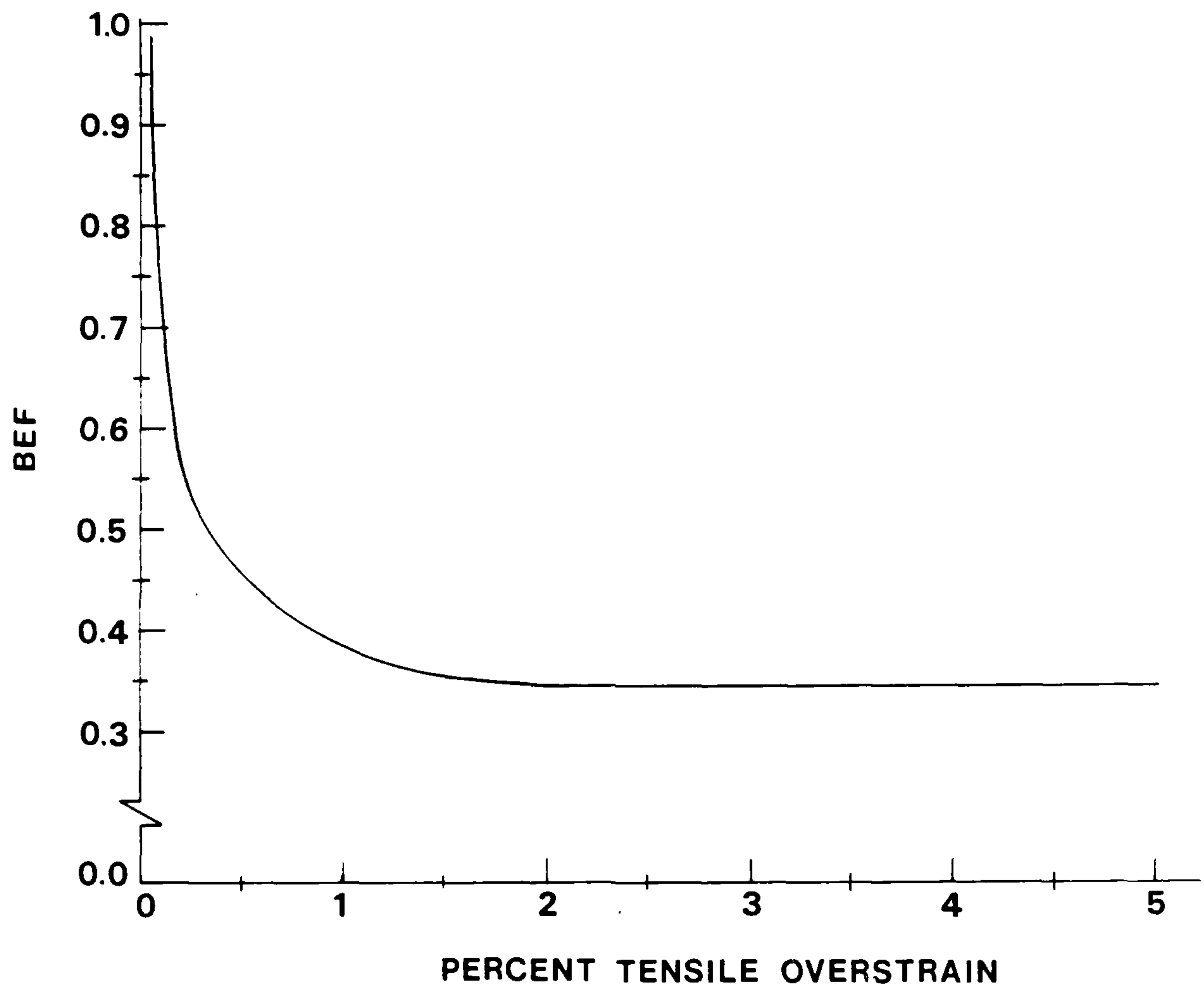

Figure 1. Bauschinger effect factor vs. percent tensile overstrain, martensitic structure of a 4330 modified steel.

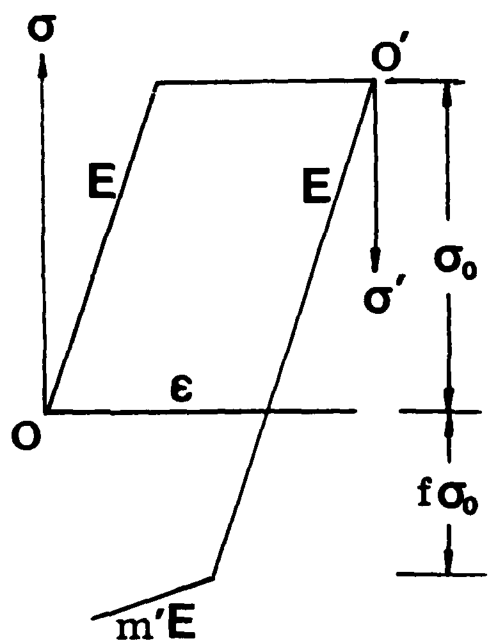

Figure 2. Stress-strain curves during loading and unloading.

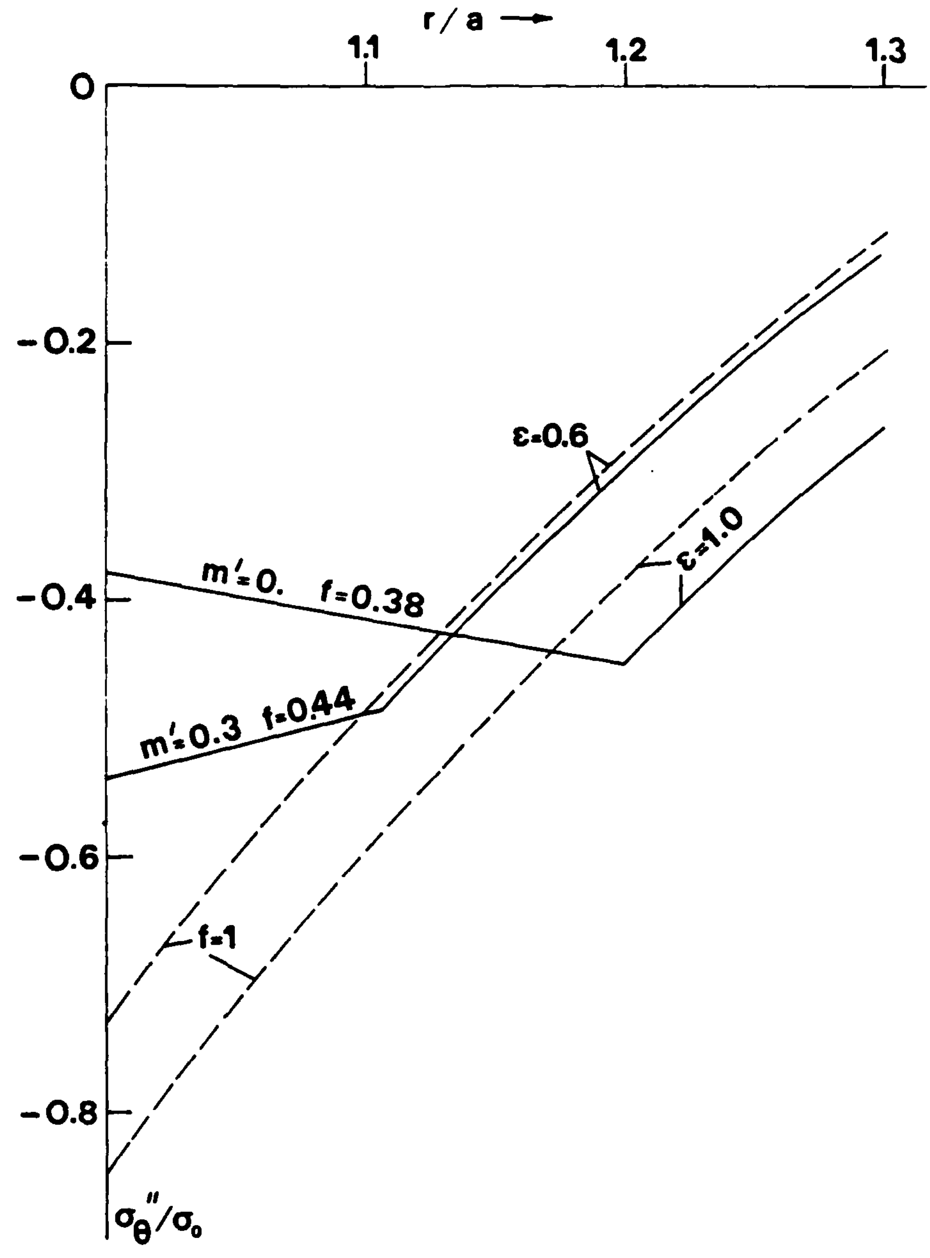

Figure 3. Dependence of σ_θ''/σ_0 on f and m' in the reverse yielding region of a cylinder of wall ratio of two.

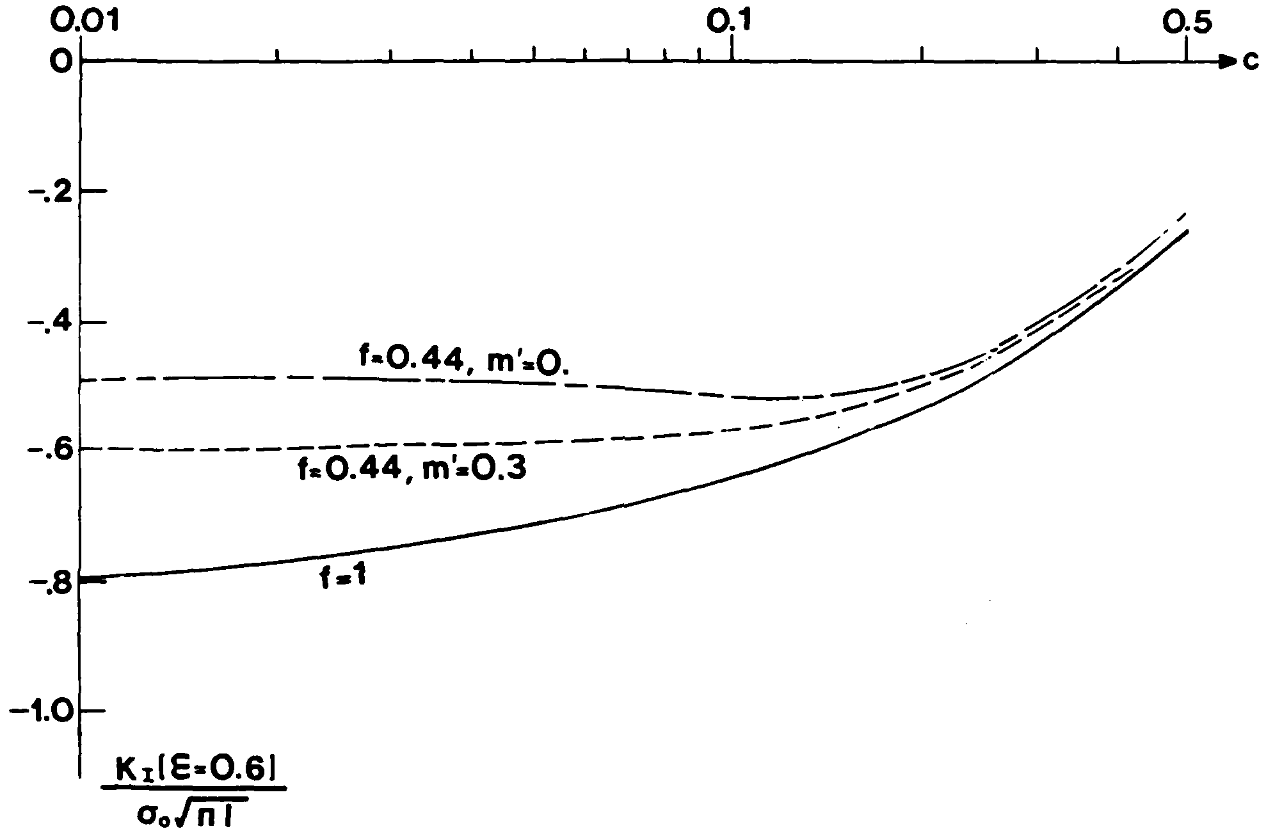

Figure 4. Dimensionless stress intensity factors as a function of dimensionless crack length c due to compressive hoop stress in a cylinder having 60 percent degree of autofrettage for various values of f and m'.

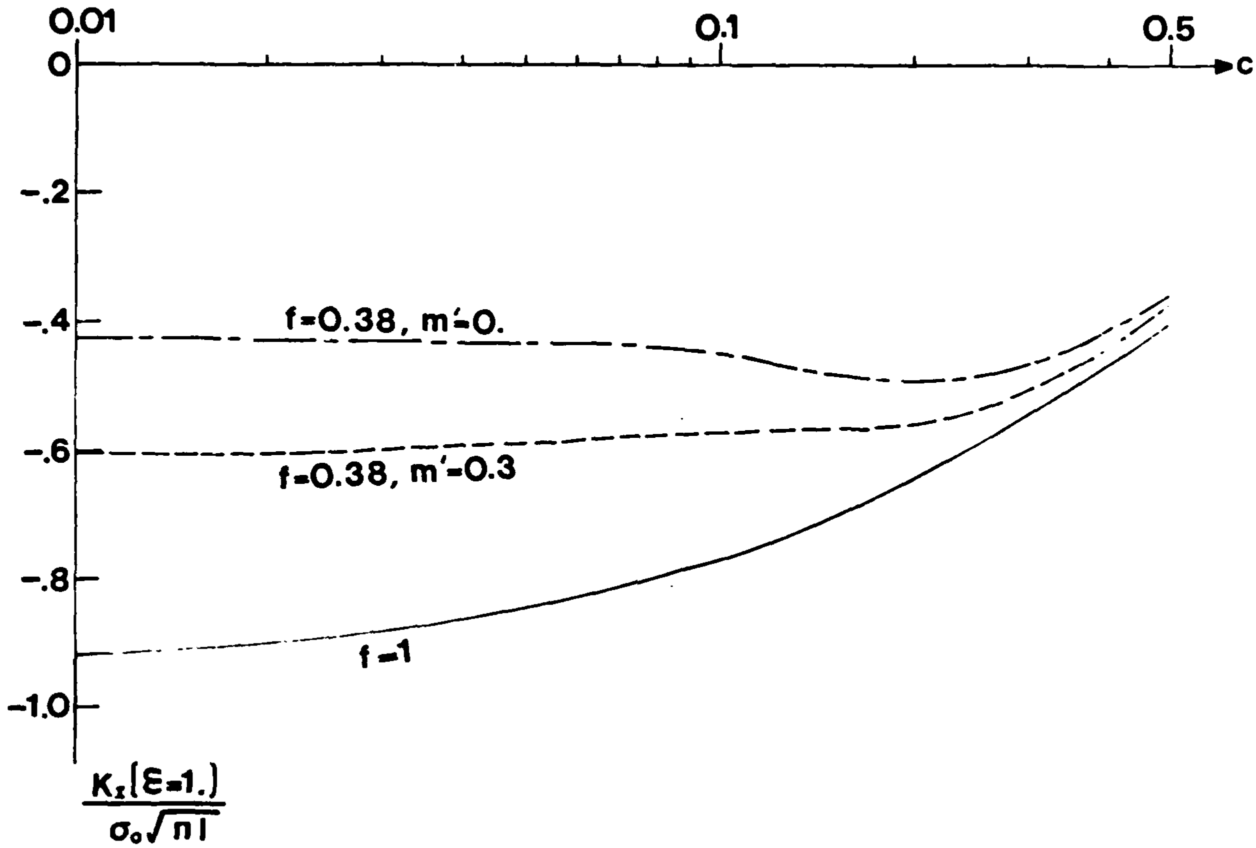

Figure 5. Dimensionless stress intensity factors as a function of dimensionless crack length c due to compressive hoop stress in a cylinder having 100 percent degree of autofrettage for various values of f and m'.

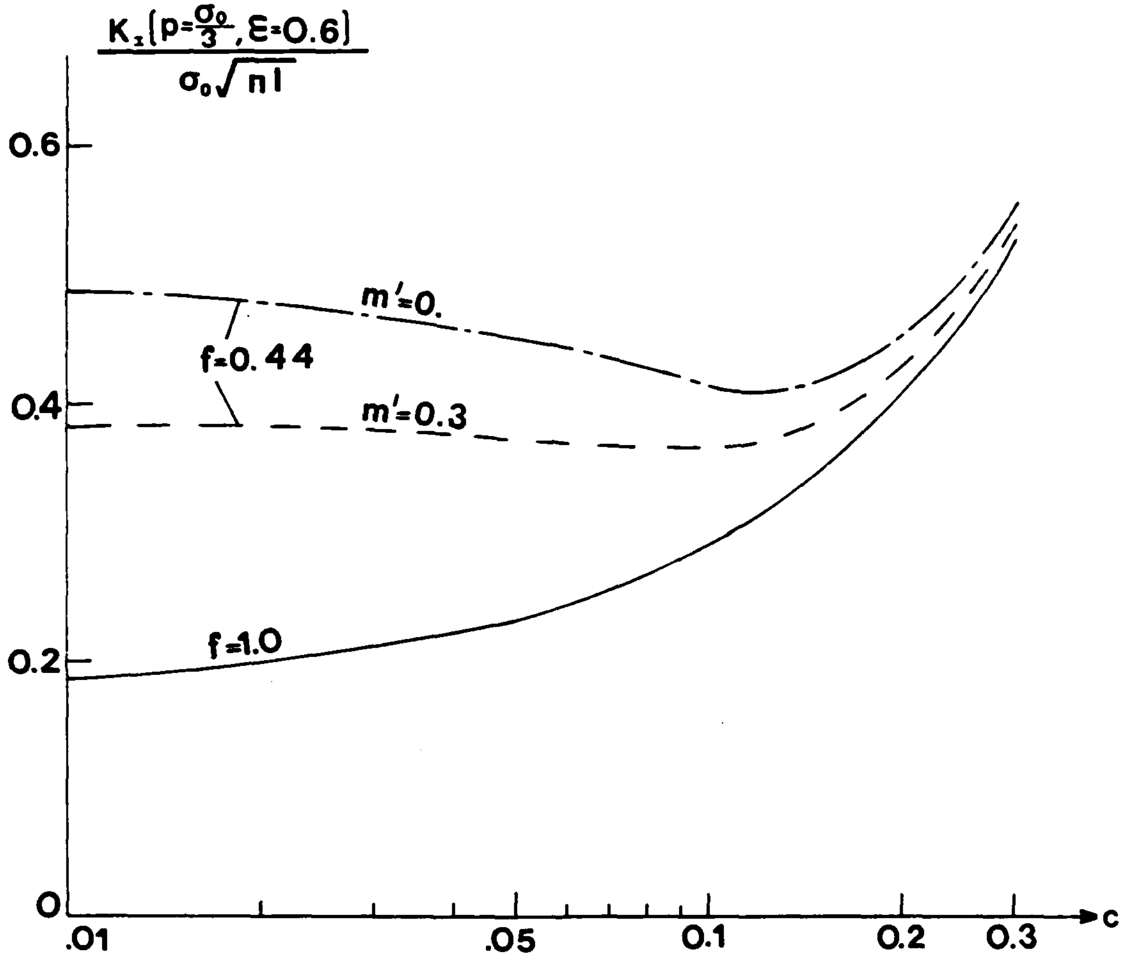

Figure 6. Resultant stress intensity factors as a function of crack length c for various values of f and m' in a pressurized, autofrettaged cylinder. Internal pressure $p = \sigma_0/3$ and degree of autofrettage $\varepsilon = 0.6$.

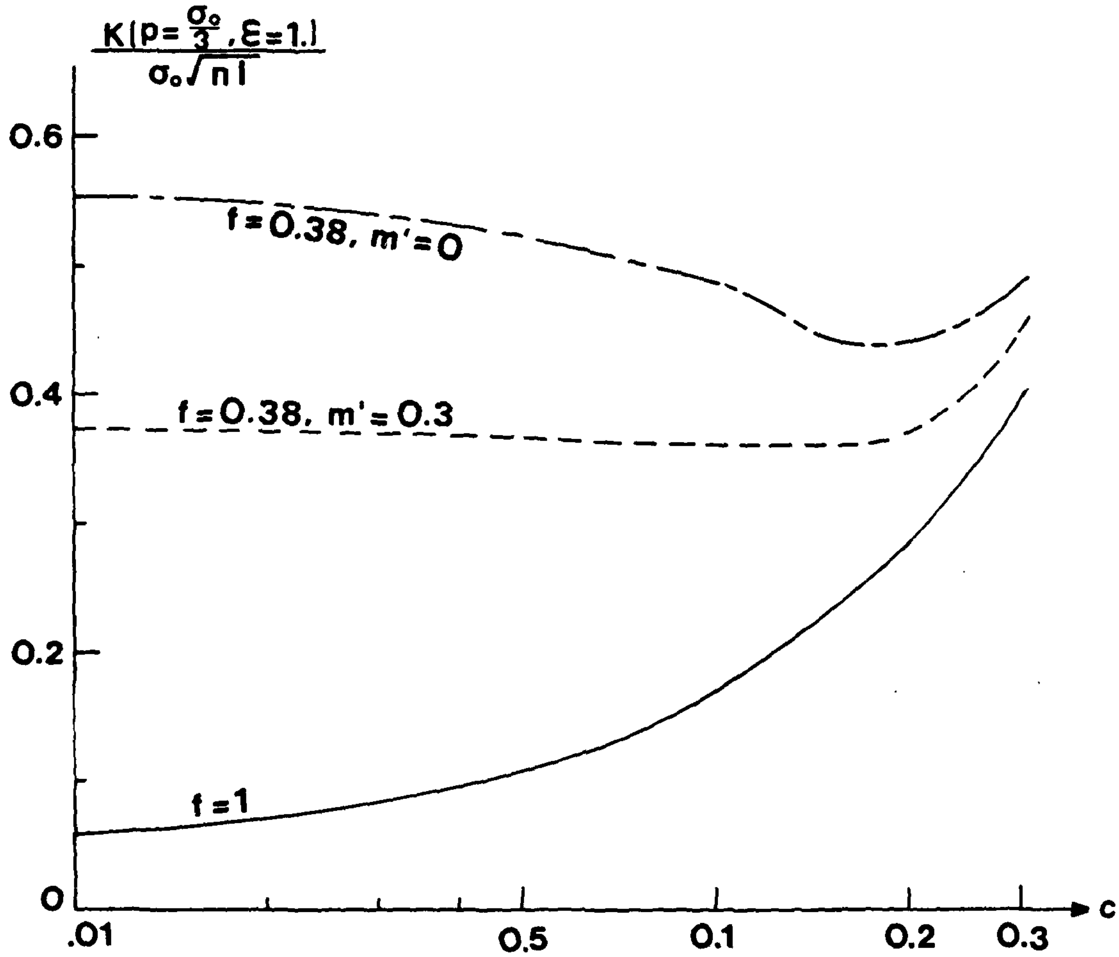

Figure 7. Resultant stress intensity factors as a function of crack length c for various values of f and m' in a pressurized, autofrettaged cylinder. Internal pressure $p = \sigma_0/3$ and degree of autofrettage $\varepsilon = 1.0$.

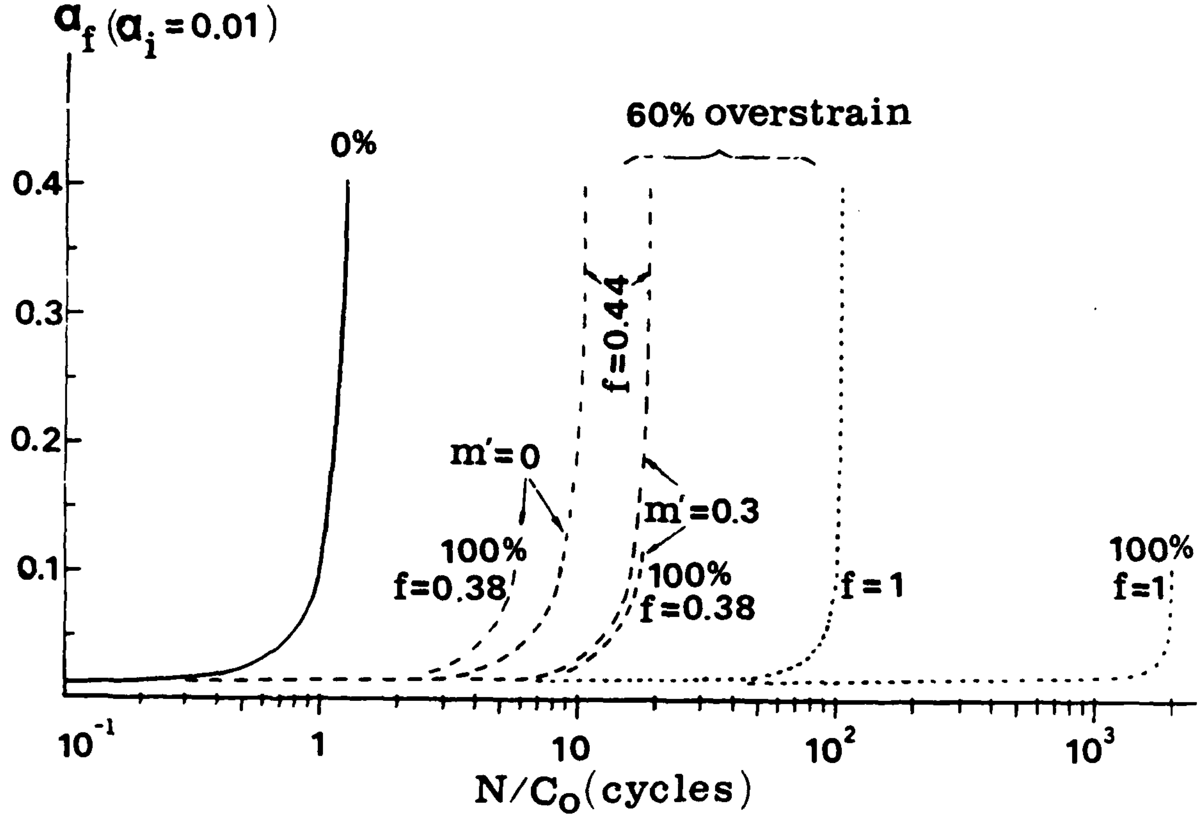

Figure 8. Resultant stress intensity factors as a function of crack length i for various values of f and m' in a pressurized, autofrettaged cylinder. Internal pressure $p = \sigma_0/1.5$ and degree of autofrettage $\epsilon = 1.0$.

APPENDIX

The definite integrals defined by Eq. (40) are explicitly given below:

$$I_{11}(\alpha,\beta) = 2(\beta^{1/2}-\alpha^{1/2})$$

$$I_{12}(\alpha,\beta) = \beta-\alpha$$

$$I_{13}(\alpha,\beta) = \frac{2}{3}(\beta^{3/2}-\alpha^{3/2})$$

$$I_{14}(\alpha,\beta) = \frac{1}{2}(\beta^{2}-\alpha^{2})$$

$$I_{21}(\alpha,\beta) = \frac{1}{\ell^2}\left[\frac{\sqrt{\beta}}{\ell_o(\ell_o-\beta)} - \frac{\sqrt{\alpha}}{\ell_o(\ell_o-\alpha)} - \frac{1}{2}\ell_o^{-3/2}\ln\left(\frac{\ell_o+\beta-2\sqrt{\ell_o\beta}}{\ell_o+\alpha-2\sqrt{\ell_o\alpha}}\,\frac{\ell_o-\alpha}{\ell_o-\beta}\right)\right]$$

$$I_{22}(\alpha,\beta) = \frac{1}{\ell^2}\left[\frac{1}{\ell_o-\beta} - \frac{1}{\ell_o-\alpha}\right]$$

$$I_{23}(\alpha,\beta) = \frac{1}{\ell^2}\left[\frac{\sqrt{\beta}}{\ell_o-\beta} - \frac{\sqrt{\alpha}}{\ell_o-\alpha} + - \ell_o^{-1/2}\ln\left(\frac{\ell_o+\beta-2\sqrt{\ell_o\beta}}{\ell_o+\alpha-2\sqrt{\ell_o\alpha}}\,\frac{\ell_o-\alpha}{\ell_o-\beta}\right)\right]$$

$$I_{24}(\alpha,\beta) = \frac{1}{\ell^2}\left[\frac{\beta}{\ell_o-\beta} - \frac{\alpha}{\ell_o-\alpha} + \ln\frac{\ell_o-\beta}{\ell_o-\alpha}\right]$$

$$I_{31}(\alpha,\beta) = (\ln\ell)I_{11}(\alpha,\beta) - 2\Big[\sqrt{\alpha}\ln(\ell_o-\alpha) - \sqrt{\beta}\ln(\ell_o-\beta) + 2(\sqrt{\beta}-\sqrt{\alpha}) +$$

$$\sqrt{\ell_o}\ln\left(\frac{\sqrt{\ell_o}+\sqrt{\alpha}}{\sqrt{\ell_o}+\sqrt{\beta}}\,\frac{\sqrt{\ell_o}-\sqrt{\beta}}{\sqrt{\ell_o}-\sqrt{\alpha}}\right)\Big]$$

$$I_{32}(\alpha,\beta) = (\ln\ell)I_{12}(\alpha,\beta) + (\ell_o-\alpha)\ln(\ell_o-\alpha) - (\ell_o-\beta)\ln(\ell_o-\beta) - (\beta-\alpha)$$

$$I_{33}(\alpha,\beta) = (\ln\ell)I_{13}(\alpha,\beta) + \frac{2}{3}\Big[\beta^{3/2}\ln(\ell_o-\beta)-\alpha^{3/2}\ln(\ell_o-\alpha)-\Big\{\frac{2}{3}(\beta^{3/2}-\alpha^{3/2}) +$$

$$+ 2\ell_o(\beta^{1/2}-\alpha^{1/2}) + \ell_o^{3/2}\ln\left(\frac{\sqrt{\ell_o}+\sqrt{\alpha}}{\sqrt{\ell_o}+\sqrt{\beta}}\,\frac{\sqrt{\ell_o}-\sqrt{\beta}}{\sqrt{\ell_o}-\sqrt{\alpha}}\right)\Big\}\Big]$$

$$I_{34}(\alpha,\beta) = (\ln\ell)I_{14}(\alpha,\beta) + \frac{1}{2}\Big[\beta^2\ln(\ell_o-\beta) - \alpha^2\ln(\ell_o-\alpha) + \ell_o^{2}\ln\frac{\ell_o-\alpha}{\ell_o-\beta} -$$

$$- 2\ell_o(\beta-\alpha) + \frac{1}{2}\{(\ell_o-\alpha^2)-(\ell_o-\beta)^2\}\Big]$$

TECHNICAL REPORT INTERNAL DISTRIBUTION LIST

	NO. OF COPIES
CHIEF, DEVELOPMENT ENGINEERING BRANCH	
ATTN: SMCAR-CCB-D	1
-DA	1
-DP	1
-DR	1
-DS (SYSTEMS)	1
-DC	1
-DM	1
CHIEF, ENGINEERING SUPPORT BRANCH	
ATTN: SMCAR-CCB-S	1
-SE	1
CHIEF, RESEARCH BRANCH	
ATTN: SMCAR-CCB-R	2
-R (ELLEN FOGARTY)	1
-RA	1
-RM	1
-RP	1
-RT	1
TECHNICAL LIBRARY ATTN: SMCAR-CCB-TL	5
TECHNICAL PUBLICATIONS & EDITING UNIT ATTN: SMCAR-CCB-TL	2
DIRECTOR, OPERATIONS DIRECTORATE	1
DIRECTOR, PROCUREMENT DIRECTORATE	1
DIRECTOR, PRODUCT ASSURANCE DIRECTORATE	1

NOTE: PLEASE NOTIFY DIRECTOR, BENET WEAPONS LABORATORY, ATTN: SMCAR-CCB-TL, OF ANY ADDRESS CHANGES.

TECHNICAL REPORT EXTERNAL DISTRIBUTION LIST

	NO. OF COPIES
ASST SEC OF THE ARMY RESEARCH & DEVELOPMENT ATTN: DEP FOR SCI & TECH THE PENTAGON WASHINGTON, D.C. 20315	1
COMMANDER DEFENSE TECHNICAL INFO CENTER ATTN: DTIC-DDA CAMERON STATION ALEXANDRIA, VA 22314	12
COMMANDER US ARMY MAT DEV & READ COMD ATTN: DRCDE-SG 5001 EISENHOWER AVE ALEXANDRIA, VA 22333	1
COMMANDER ARMAMENT RES & DEV CTR US ARMY AMCCOM ATTN: SMCAR-FS	1
SMCAR-FSA	1
SMCAR-FSM	1
SMCAR-FSS	1
SMCAR-AEE	1
SMCAR-AES	1
SMCAR-AET-O (PLASTECH)	1
SMCAR-MSI (STINFO) DOVER, NJ 07801	2
DIRECTOR BALLISTICS RESEARCH LABORATORY ATTN: AMXBR-TSB-S (STINFO) ABERDEEN PROVING GROUND, MD 21005	1
MATERIEL SYSTEMS ANALYSIS ACTV ATTN: DRXSY-MP ABERDEEN PROVING GROUND, MD 21005	1

	NO. OF COPIES
COMMANDER US ARMY AMCCOM ATTN: SMCAR-ESP-L ROCK ISLAND, IL 61299	1
COMMANDER ROCK ISLAND ARSENAL ATTN: SMCRI-ENM (MAT SCI DIV) ROCK ISLAND, IL 61299	1
DIRECTOR US ARMY INDUSTRIAL BASE ENG ACTV ATTN: DRXIB-M ROCK ISLAND, IL 61299	1
COMMANDER US ARMY TANK-AUTMV R&D COMD ATTN: TECH LIB - DRSTA-TSL WARREN, MI 48090	1
COMMANDER US ARMY TANK-AUTMV COMD ATTN: DRSTA-RC WARREN, MI 48090	1
COMMANDER US MILITARY ACADEMY ATTN: CHMN, MECH ENGR DEPT WEST POINT, NY 10996	1
US ARMY MISSILE COMD REDSTONE SCIENTIFIC INFO CTR ATTN: DOCUMENTS SECT, BLDG. 4484 REDSTONE ARSENAL, AL 35898	2
COMMANDER US ARMY FGN SCIENCE & TECH CTR ATTN: DRXST-SD 220 7TH STREET, N.E. CHARLOTTESVILLE, VA 22901	1

NOTE: PLEASE NOTIFY COMMANDER, ARMAMENT RESEARCH, DEVELOPMENT, AND ENGINEERING CENTER, US ARMY AMCCOM, ATTN: BENET WEAPONS LABORATORY, SMCAR-CCB-TL, WATERVLIET, NY 12189-4050, OF ANY ADDRESS CHANGES.

TECHNICAL REPORT EXTERNAL DISTRIBUTION LIST (CONT'D)

	NO. OF COPIES
COMMANDER US ARMY LABCOM MATERIALS TECHNOLOGY LAB ATTN: SLCMT-IML WATERTOWN, MA 01272	2
COMMANDER US ARMY RESEARCH OFFICE ATTN: CHIEF, IPO P.O. BOX 12211 RESEARCH TRIANGLE PARK, NC 27709	1
COMMANDER US ARMY HARRY DIAMOND LAB ATTN: TECH LIB 2800 POWDER MILL ROAD ADELPHIA, MD 20783	1
COMMANDER NAVAL SURFACE WEAPONS CTR ATTN: TECHNICAL LIBRARY CODE X212 DAHLGREN, VA 22448	1

	NO. OF COPIES
DIRECTOR US NAVAL RESEARCH LAB ATTN: DIR, MECH DIV CODE 26-27, (DOC LIB) WASHINGTON, D.C. 20375	1 1
COMMANDER AIR FORCE ARMAMENT LABORATORY ATTN: AFATL/MN AFATL/MNG EGLIN AFB, FL 32542-5000	1 1
METALS & CERAMICS INFO CTR BATTELLE COLUMBUS LAB 505 KING AVENUE COLUMBUS, OH 43201	1

<u>NOTE</u>: PLEASE NOTIFY COMMANDER, ARMAMENT RESEARCH, DEVELOPMENT, AND ENGINEERING CENTER, US ARMY AMCCOM, ATTN: BENET WEAPONS LABORATORY, SMCAR-CCB-TL, WATERVLIET, NY 12189-4050, OF ANY ADDRESS CHANGES.

END

1-87

DTIC